Aerosol and Air Quality Research, 16: 2287–2293, 2016

ISSN: 1680-8584 print / 2071-1409 online
doi: 10.4209/aaqr.2016.03.0126

Acid Mist Cyclone Separation Experiment on the Hydrochloric Acid Regeneration System of a Cold Rolling Steel Plant

Yan-Hong Zhang, An-Lin Liu, Liang Ma*, Yi-Mou Wang

School of Mechanical and Power Engineering, East China University of Science and Technology, Shanghai 200237, China

ABSTRACT

In the hydrochloric acid regeneration system of a cold rolling steel plant, the large amounts of hydrochloric acid droplets and iron oxide dust in the flue gas at the absorption column outlet cause serious air pollution. To reduce pollution, a high-precision cyclone separator is utilized to recycle hydrogen chloride acid mist and iron oxide dust simultaneously. The key factors of the high-precision cyclone separator, such as pressure drop, separation efficiency, and fluid density, are investigated to determine the optimal operation parameters under practical working conditions. Results show that the separation efficiency of the cyclone separator increases rapidly initially and then decreases gradually with an increase in pressure drop. Pressure drop and separation efficiency increase slightly with an increase in inlet fluid concentration. When the velocities of the inlet gas are 4.8–10 m s^{-1} and 5.0–9.2 m s^{-1}, the separation efficiencies of hydrochloric acid and iron oxide are both higher than 80%. When the velocity of the inlet gas is 6.67 m s^{-1}, the separation efficiencies of hydrochloric acid and iron oxide reach the highest values of 92% and 89%, respectively.

Keywords: Flue gas purification; Cold rolling steel plant; Hydrochloric acid regeneration; Cyclone separator; Separation performance.

INTRODUCTION

With the continuously improving requirements of energy conservation and environmental protection, industrial emission standards have become increasingly stringent. Hydrochloric acid regeneration devices in early-founded cold rolling steel plants need to be improved to adapt to the new emission standards of the steel rolling industry. In the existing production process, flue gas that contains hydrochloric acid mist and iron oxide dust is often transmitted to downstream equipment or is discharged into the atmosphere directly after being washed. The purification effect of the column washer for flue gas is not good and results in downstream equipment corrosion and excessive exhaust emission. Therefore, reducing the amount of hydrochloric acid mist and iron oxide dust in flue gas emission is highly significant for emission reduction and improvement of the efficiency of acid regeneration systems. Gravity settler cannot capture the fine particles which lest than 10 μm in flue gas. Although demist nets can capture fine particles, fouling and plugging often occur. Furthermore, these nets are unsuitable for situations involving high liquid content. By contrast, a cyclone separator, which has a simple structure and stable performance, can separate fine particles. In addition, it does not become blocked easily (Movafaghian *et al.*, 2000; Wang *et al.*, 2010). With the continuous development of computer simulation technology, the computational fluid dynamics (CFD) technology has been applied to calculate the gas flow field in a cyclone separator with different entrance structure, the results showed that the effect of changing the inlet width was more significant than changing the inlet height (Elsayed and Lacor, 2011a, b; Avci *et al.*, 2013). By comparing with the conventional models which include the theoretical and statistical models as well as the artificial neural network model, Chen and Shi (2007) established a universal model to calculate cyclone pressure drop. Zhao (2009, 2010, 2012) found that the SVM (support vector machine) model provides the higher generalization performance in pressure drop. Li *et al.* (2015) established a new pressure drop model which indicates this pressure drop model was suitable for the cyclone splitters with pure or droplet-laden gases. Tsai *et al.* (2004, 2007, 2011) remove nanoparticles in low pressure or vacuum conditions by an axial-flow cyclone. Quan *et al.* (2009, 2010) invented a new type of gas-liquid stripping equipment-the water jet air cyclone separator (WSA) which greatly improves the efficiency of the stripping of ammonia. Yang *et al.* (2015) established an innovative operation mode to a new pressure drop model of gas - liquid cyclone. Zhang *et al.* (2015) calculated the residence time distribution in short-

* Corresponding author.
Tel.: +86-021-64252748; Fax: +86-021-64251894
E-mail address: maliang@ecust.edu.cn

contact cyclone reactors by CFD simulation and experiment. Ma *et al.* (2013, 2014a, b, 2015) applied the micro cyclone to the ultra-high pressure environment of removing hydrocarbon or ammonia in recycle hydrogen, compared with the traditional gas-liquid separation device has a better effect.

Many scholars have investigated the high-precision cyclone separator in many aspects, but no study has been conducted on the high-precision cyclone separator in the hydrochloric acid regeneration system of a cold rolling steel plant. In consideration of the process conditions of a hydrochloric acid regeneration system, we design a high-precision cyclone separator. An industrial sideline test is conducted to measure the effects of several factors (e.g., pressure drop and separation efficiency) on separation performance, determine the optimum operation parameters for the high-precision cyclone separator, and effectively remove hydrogen chloride acid droplets and iron oxide dust in flue gas.

METHODS

The high-precision cyclone separator adopted in the experiment is a rectangular tangential inlet micro cyclone separator, as shown in Fig. 1. The material of cyclone separator is Fiber Reinforced Plastics (FRP), and the dimension parameters (mm) are as follows: D = 70, a = 50, b = 20, di = 32, dc = 32, s = 100, H_1 = 150, H_2 = 225, H_3 = 150, I_n = 150. The separator was optimized based on the Stairmand high-efficiency cyclone. The diameter of the cylindrical section of the cyclone separator was reduced, centrifugation was enhanced, and a parallel guide plate was added to the inlet to make the air flow smooth.

The industry sideline experimental flow chart is shown in Fig. 2. Waste hydrochloric acid is regenerated and recycled through the reactor (1). Waste acid, with SiO_2 removed, enters the preconcentrator for heating concentration. Concentrated waste acid is expelled from the pump to the reactor for Ruthner spray, and Fe_2O_3 powder is generated from this reaction. Dust particles with a small diameter enter the low-precision cyclone separator (2) for the separation of HCl and Fe_2O_3 and then go into the preconcentrator (3). After cooling and dust removal, they enter the absorption column (4). By spraying rinsing water at the top of the absorption column, HCl gas is absorbed and changed to regenerated acid. With the help of the fan (8), the flue gas exhausted by the absorption column enters the high-precision cyclone separator (7). Fine hydrogen chloride acid mist droplets and iron oxide dust particles are then further separated. The flue gas from the overflow port of the high-precision cyclone separator (7) is washed in the column washer (5) and then exhausted into the atmosphere. The separating medium at the bottom flow port is discharged with regenerated acid.

The experimental device is shown in the line box of Fig. 2. During the experiment, gas samples in the inlet and separating medium samples at the underflow port of the high-precision cyclone separator were obtained and measured. The contents of Fe_2O_3 and HCl were measured with a plasma emission spectrometer and an ion chromatographer, respectively. In unit time, the total amount in the inlet is g_i, the total collection at the underflow port is g_u, and separation efficiency E can be represented as $E = g_u/g_i$.

Experimental Materials

The temperature of the flue gas extracted from the experimental site was approximately 78°C. The content of steam, N_2, CO_2, O_2, and HCl in flue gas was 71.44%, 22.83%, 4.66%, 0.9%, and 0.17% respectively. The variation range of water droplets concentration in the flue gas was 179–283 g m^{-3}, that of Fe_2O_3 concentration was 460–600 mg m^{-3}, and that of HCl concentration was 2070–2680 mg m^{-3}. Fe_2O_3 in flue gas is reddish brown, insoluble in water, and does not react with water. Hydrogen chloride has a suffocating odor, and its density is higher than that of air. Its aqueous solution is hydrochloric acid, which can corrode downstream devices and pollute air if exhausted into it. The Fe_2O_3 can react with HCl in the flue gas and separated liquid. The HCl react with Fe_2O_3 to $FeCl_3$, and dissolved in the solution,

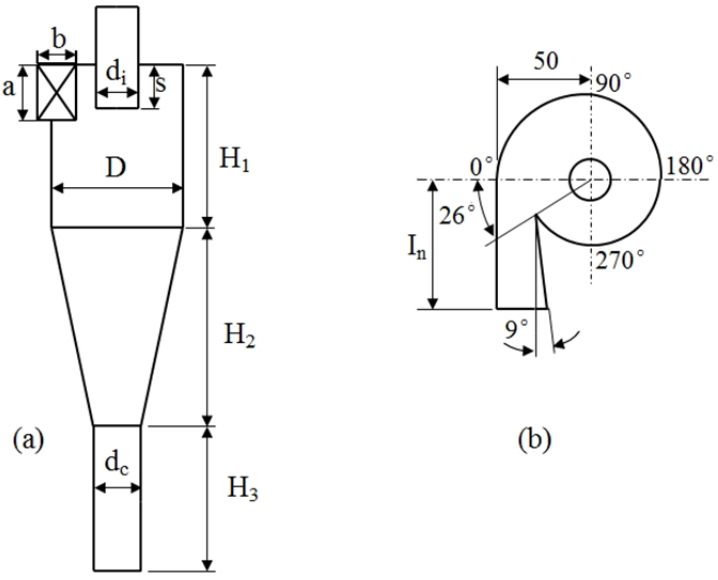

Fig. 1. high-precision Cyclone structure (a) and angular positions (b).

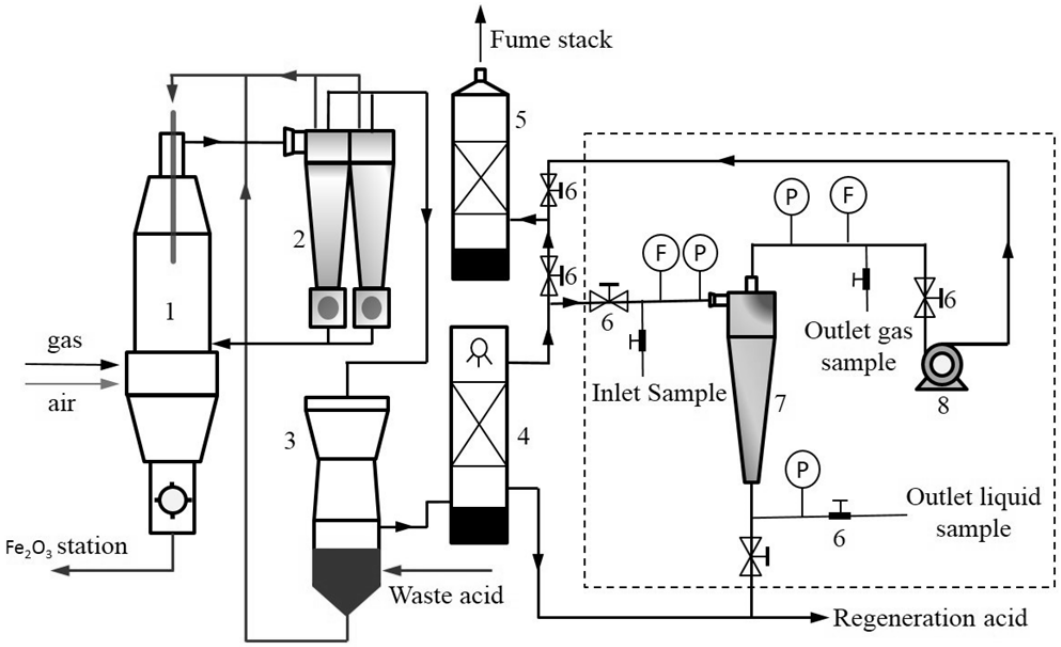

1. Reactor 2. Low precision cyclone separator 3. Preconcentrator 4. Absorption column
5. Column washer 6. Cut-off valve 7. High precision cyclone separator 8. Fan

Fig. 2. Flow chart of the experiment.

which was separated and collected by cyclone, and the remaining part of the Fe_2O_3 exists in the form of solid particles in the solution. We can get weight of this part of Fe_2O_3 particles by filtration. With further evaporation of the filtrate, we can get the weight of $FeCl_3$, and then the total weight of Fe_2O_3 particles can be obtained by the conservation of Fe^{3+}. The gravimetric method was applied to measure the content of water droplets and Fe_2O_3 in flue gas. First, a membrane filter is connected to the sampling port (precision > 0.1 mg m^{-3}, particles size > 0.01 μm), through the flow time and flow rate we can obtain the amount of gas (m^3) which flow through the membrane filter. Second, we can get the increased weight (particles and water droplets) of membrane filter by electronic balance. Third, the weight of Fe_2O_3 particles can be obtained by filtration, and we can get the weight of $FeCl_3$ and water droplet by further evaporation.

A Melvin droplet and particle size analyzer was utilized to determine the diameter of the Fe_2O_3 particle in hydrochloric acid liquid. The measured average diameter of Fe_2O_3 dust was 1.796 μm, and the diameter of more than 90% of the particles was larger than 0.502 μm. The Fe_2O_3 particle size–volume curve is shown in Fig. 3, and the Fe_2O_3 SEM image is shown in Fig. 4.

Experimental Results and Discussion

As for the industrial application of the high-precision cyclone separator, we mainly investigated pressure drop and separation efficiency. A small pressure drop can reduce energy consumption, and the system fan need not be modified when installing the cyclone separating device. A fluctuation in flue gas flow occurs in the industrial production. This fluctuation affects the pressure drop and separation efficiency of the high-precision cyclone separator. Based on previous engineering designs and uses, we selected the flue gas velocity of 4.167–11.677 m s^{-1} as the experimental range.

When the inlet droplet concentration was 263 g m^{-3}, we measured the pressure difference ΔP in the cyclone separator inlet and overflow port. The flue gas velocity in the inlet was changed. The effect of different velocities in the inlet on droplet separation efficiency and pressure drop was tested, and the results are shown in Fig. 5. The ΔP increases with an increase in inlet velocity V_{in}, and the increase rate is rapid. The separation efficiency of the droplets in the flue gas increases initially and then decreases with an increase in gas velocity in the inlet of the cyclone separator. When the gas velocity in the cyclone separator is low, centrifugal force reduces the migration velocity of droplets to the side wall, and the droplets far from the wall are brought out by gas before separation. With an increase in the inlet flow rate, the centrifugal force of droplets increases, and the droplets move fast to the side wall. During this process, the droplets form larger droplets because of collision and coalescence; these larger droplets are easy to separate. Thus, the separation rate increases rapidly. As the gas flow rate continues to increase, the droplet collision and shear breaking effects increase. A large number of small droplets is formed. These droplets are discharged with the internal circulating flow, resulting in low separation efficiency. The increased flow velocity results in a short retention period of droplets in the separation zone, which in turn leads to increased short-circuit flow. The droplet separation efficiency of the cyclone separator is high and can reach up to 95%. The area with separation efficiency higher than 80% is considered a highly efficient separation zone. The variation range of the highly efficient separation zone can reach 4.4–10.3 m s^{-1}.

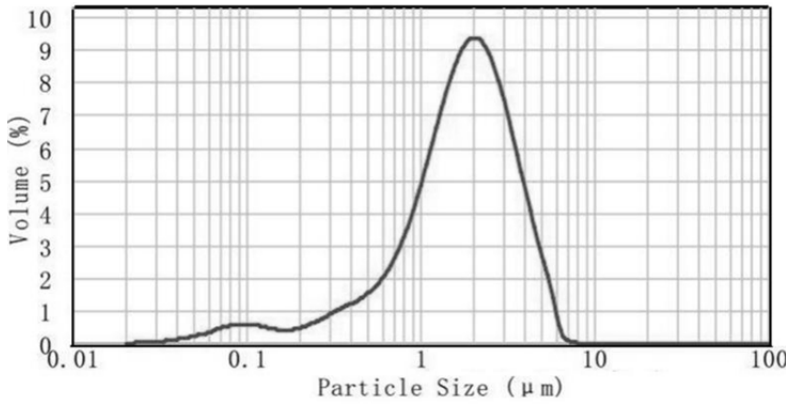

Fig. 3. Fe_2O_3 particle size–volume curve.

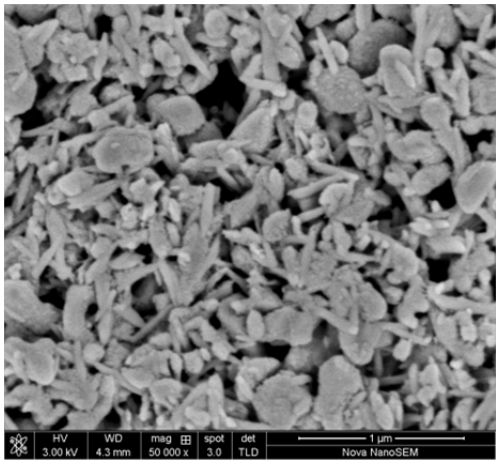

Fig. 4. Fe_2O_3 SEM image.

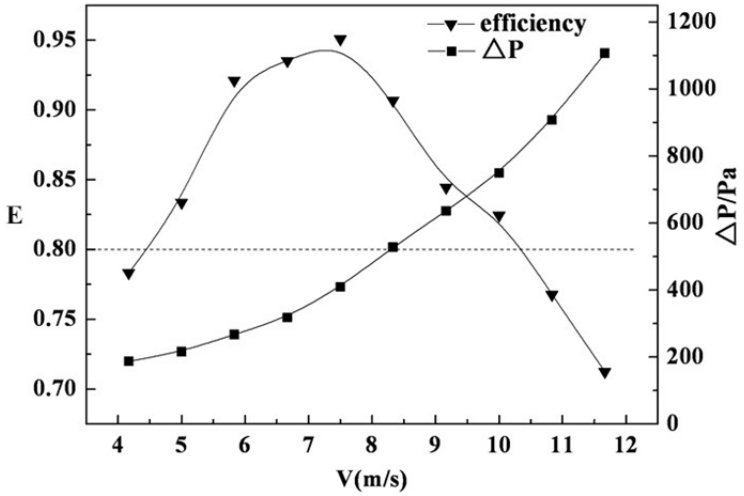

Fig. 5. Relationship of E, ΔP, and V_{in}. C_i: 230–250 g m^{-3}, C_{Fe2O3}: 540–560 mg m^{-3}, C_{HCl}: 2300–2500 mg m^{-3}, P_{in} = 0.23 MPa, temperature 78°C.

In the actual production process, the frequency control of the system fan changes according to the working condition to adapt to the process. This situation requires the cyclone separator to be flexible to some extent. The system fan flow rate can change fluid concentration C_i in flue gas. Therefore, the effect of inlet fluid concentration on separation performance needs to be investigated. The relationship between pressure drop at the overflow port and fluid concentration at different inlet flow velocities was tested in this study. The results are shown in Fig. 6. Pressure drop

increases slightly with an increase in concentration. When the velocity at the inlet is 11.67 m s^{-1}, the pressure drop increase is the largest (only 3.5%). The increased pressure drop is mainly caused by the increase in internal rotation loss in the cyclone separator because an increase in liquid concentration in flue gas increases the viscosity and density of gas–liquid two-phase flow in the cyclone separator's inlet. Thus, if the fluid concentration in the cyclone separator's inlet is in the range of 179–283 g m^{-3}, it would have minimal impact on the pressure drop of the cyclone separator.

The most important indicator utilized in acid regeneration by a cyclone separator is the separation efficiency for Fe_2O_3 and HCl. Five groups of experiments were conducted at different velocities. In each experimental period, the average concentrations of Fe_2O_3 and HCl in the inlet and outlet and the corresponding separation efficiency were measured. The results are shown in Figs. 7 and 8. The concentration of Fe_2O_3 and HCl in the inlet fluctuates. Comparison of the concentrations in the inlet and outlet indicates that the flue gas purification effect by the cyclone separator is obvious. The velocity ranges in the highly efficient zones of Fe_2O_3 and HCl are 5.00–9.17 m s^{-1} and 5.00–9.72 m s^{-1}, respectively. When the velocity is 6.67 m s^{-1}, the highest separation efficiencies are 89% and 92%.

With 280 working days a year and average cyclone separation efficiency of 85%, each acid separation station can directly separate 32.5 t of ferric oxide powder and 145.8 t of hydrogen chloride. Thus, the workload of the column washer is reduced significantly, and a substantial amount of resources is recycled.

Fig. 9 shows the relationship curve of concentration and separation efficiency at different velocities at the inlet, namely, 5.00, 6.67, and 11.67 m s^{-1}. With an increase in fluid concentration, separation efficiency increases slightly. When the velocities are 5.00, 6.67, and 8.33 m s^{-1}, the corresponding increments are 3.6%, 3.0%, and 2.2%, respectively. With an increase in inlet velocity, the increase in separation efficiency becomes small. This result shows that at a high velocity, the influence of droplet breakage on separation efficiency increases.

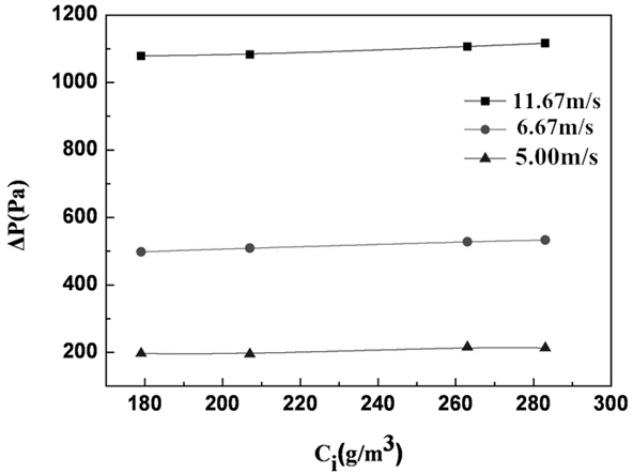

Fig. 6. Relationship of ΔP and C_i at different V_{in}. C_{Fe2O3}: 540–560 mg m^{-3}, C_{HCl}: 2300–2500 mg m^{-3}, P_{in} = 0.23 MPa, temperature 78°C.

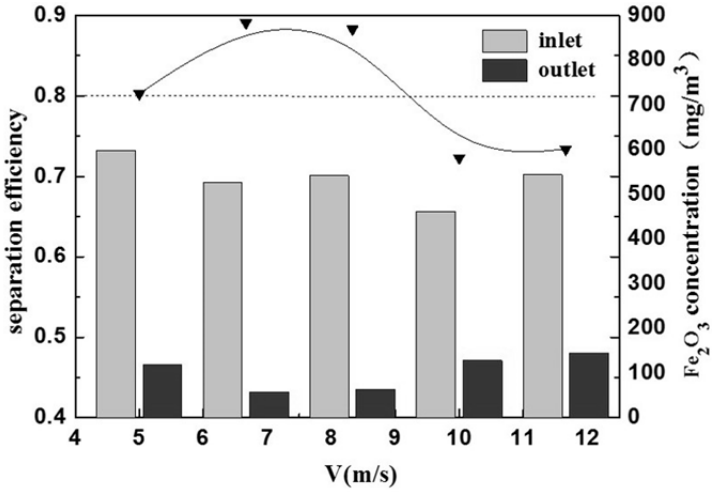

Fig. 7. Relationship of inlet and outlet Fe_2O_3 concentration, E, and V_{in}. C_i: 230–250 g m^{-3}, C_{HCl}: 2300–2500 mg m^{-3}, P_{in} = 0.23 MPa, temperature 78°C.

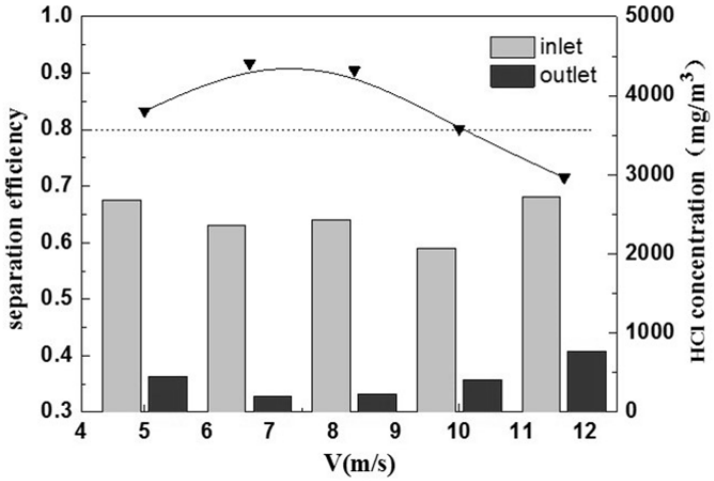

Fig. 8. Relationship of inlet and outlet HCl concentration, E, and V_{in}. C_i: 230–250 g m^{-3}, C_{Fe2O3}: 540–560 mg m^{-3}, P_{in} = 0.23 MPa, temperature 78°C.

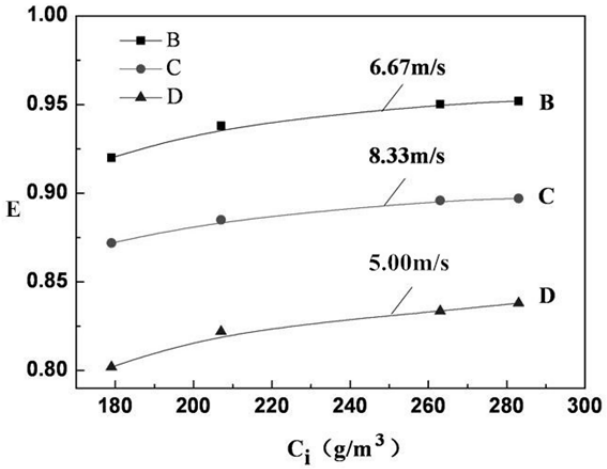

Fig. 9. Relationship of E and C_i at different V_{in}. C_{Fe2O3}: 540–560 mg m^{-3}, C_{HCl}: 2300–2500 mg m^{-3}, P_{in} = 0.23 MPa, temperature 78°C.

CONCLUSIONS

When the inlet liquid content of the cyclone separator is 263 g m^{-3}, the separation efficiency of acid fog droplets in the cyclone separator increases initially and then decreases with an increase in pressure drop. The velocity in the highly efficient zone of the cyclone separator to separate droplets is 5.00–10.3 m s^{-1}, and the corresponding pressure drop at the overflow port is 0.20–0.82 KPa. When the velocity is 6.67 m s^{-1}, droplet separation efficiency reaches the highest value of 95%, and the corresponding pressure drop is 0.32 KPa. At the same time the highest separation efficiency of Fe_2O_3 and HCl is 89% and 92%, respectively. Within 179–283 g m^{-3}, the increase in fluid concentration in the cyclone separator inlet causes a slight increase in pressure drop at the overflow port and droplet separation efficiency, with the largest increments of 3.5% and 3.6%, respectively. This result shows that the cyclone separator has wide operation flexibility. With 280 working days a year and average cyclone separation efficiency of 85%, each acid separation station can directly separate 32.5t of ferric oxide powder and 145.8t of hydrogen chloride.

ACKNOWLEDGMENTS

We would like to express our thanks for the sponsorship of the National Key Research and Development Program of China (2016YFC0204500), the Fundamental Research Funds for the Central Universities (22A201514028), the China Postdoctoral Science Foundation (2015M571505).

SYMBOLS USED

a	[mm]	cyclone inlet height
b	[mm]	cyclone inlet width
C_i	[g m^{-3}]	droplet concentration
d_i	[mm]	cyclone vortex finder diameter
d_c	[mm]	cyclone conical liquid outlet diameter
D	[mm]	gas outlet of the device
E	[-]	separation efficiency

g_u	[kg s^{-1}]	droplet concentration of inlet air
g_i	[kg s^{-1}]	droplet concentration of overflow air
H_1	[mm]	cyclone cylindrical body height
H_2	[mm]	cyclone conical body height
H_3	[mm]	cyclone underflow pipe height
I_n	[mm]	cyclone inlet length
ΔP	[Pa]	pressure drop between inlet and overflow
S	[mm]	extrusive vortex finder height
V_{in}	[m s^{-1}]	victory of inlet
θ	[°]	cone angle
C_{Fe2O3}	[mg m^{-3}]	Fe_2O_3 concentration in gas
C_{HCl}	[mg m^{-3}]	HCl concentration in gas
P_{in}	[MPa]	inlet pressure of cyclone

REFERENCES

Avci, A., Karagoz, I. and Surmen, A. (2013). Development of a new method for evaluating vortex length in reversed flow cyclone separators. *Powder Technol*. 235: 460–466.

Chen, J. and Shi, M. (2007). A universal model to calculate cyclone pressure drop. *Powder Technol.* 171: 184–191.

Elsayed, K. and Lacor, C. (2011a). Numerical modeling of the flow field and performance in cyclones of different come-tip diameters. *Comput. Fluids* 51: 48–59.

Elsayed, K. and Lacor, C. (2011b). The effect of cyclone inlet dimensions on the flow pattern and performance. *Appl. Math. Modell.* 35: 1952–1968.

Li, Q., Xu, W.W., Wang, J.J. and Jin, Y.H. (2015). Performance evaluation of a new cyclone separator – Part I experimental results. *Sep. Purif. Technol.* 141: 53–58.

Ma, L., Yang, Q., Huang, Y., Qian, P. and Wang, J.G. (2013). Pilot test on the removal of coke powder from quench oil using a hydrocyclone. *Chem. Eng. Technol*. 36: 696–702.

Ma, L., Shen, Q., Li, J., Zhang, Y., Wu, J. and Wang, H. (2014a). Efficient gas-liquid cyclone device for recycled hydrogen in a hydrogenation unit. *Chem. Eng. Technol*. 37: 1072–1078.

Ma, L., Wu, J., Zhang, Y., Shen, Q., Li, J. and Wang, H. (2014b). Study and application of a cyclone for removing amine droplets from recycled hydrogen in a hydrogenation unit. *Aerosol Air Qual. Res.* 14: 1675–1684.

Ma, L., Fu, P., Wu, J., Wang, F., Li, J., Shen, Q. and Wang, H. (2015). CFD simulation study on particle arrangements at the entrance to a swirling flow field for improving the separation efficiency of cyclone. *Aerosol Air Qual. Res.* 15: 2456–2465.

Movafaghian, S., Jaua-Marturet, J.A., Mohan, R.S., Shoham, O. and Kouba, G.E. (2000). The effects of geometry, fluid properties and pressure on the hydrodynamics of gas–liquid cylindrical cyclone separators. *Int. J. Multiphase Flow* 26: 999–1018.

Quan, X., Wang, F., Zhao, Q., Zhao, T. and Xiang, J. (2009). Air stripping of ammonia in a water-sparged aerocyclone reactor. *J. Hazard. Mater*. 170: 983–988.

Quan, X., Ye, C., Xiong, Y., Xiang, J. and Wang, F. (2010). Simultaneous removal of ammonia, P and COD from anaerobically digested piggery wastewater using an integrated process of chemical precipitation and air stripping. *J. Hazard. Mater*. 178: 326–332.

Tsai, C.J., Chen, D.R., Chein, H.M., Chen, S.C., Roth, J.L., Hsu, Y.D., Li, W.L. and Biswas, P. (2004). Theoretical and experimental study of an axial flow cyclone for fine particle removal in vacuum conditions. *J. Aerosol. Sci*. 35: 1105–1118.

Tsai, C.J., Chen, S.C., Przekop, R. and Moskal, A. (2007). Study of an axial flow cyclone to remove nanoparticles in vacuum. *Environ. Sci. Technol.* 41: 1689–1695.

Tsai, C.J., Huang, C.Y., Chen, S.C., Ho, C.E., Huang, C.H., Chen, C.W., Chang, C.P., Tsai, S.J. and Ellenbecker, M.J. (2011). Exposure assessment of nano-sized and respirable particles at different workplaces. *J. Nanopart. Res.* 41: 61–72.

Wang, S.B., Gomez, L., Mohan, R., Shoham, O., Kouba, G. and Marrelli, J. (2010). The state-of-the-art of gas-liquid cylindrical cyclone control technology: From laboratory to field. *J. Energy Res. Technol.* 132: 032701.

Yang, J., Liu, C., Li, S., Sun, B., Xiao, J. and Jin, Y. (2015). A new pressure drop model of gas–liquid cyclone with innovative operation mode. *Chem. Eng. Process.* 95: 256–266.

Zhang, Y., Wang, Z., Jin, Y., Li, Z. and Yi, W. (2015). CFD simulation and experiment of residence time distribution in short-contact cyclone reactors. *Adv. Powder Technol.* 26: 1134–1142.

Zhao, B. (2009). Modeling pressure drop coefficient for cyclone separators: A support vector machine approach. *Chem. Eng. Sci.* 64: 4131–4136.

Zhao, B. (2010). Development of a dimensionless logistic model for predicting cyclone separation efficiency. *Aerosol Sci. Technol.* 44: 1105–1112.

Zhao, B. (2012). Prediction of gas-particle separation efficiency for cyclones: A time-of-flight model. *Sep. Purif. Technol.* 85: 171–177.

Received for review, May 12, 2016
Revised, July 13, 2016
Accepted, August 23, 2016